https://doi.org/10.15407/ujpe70.11.753

V.I. ZHDANOV [1, 2]

[1] Astronomical Observatory, Taras Shevchenko National University of Kyiv
(3, Observatorna Str., Kyiv 04053, Ukraine)
[2] Applied Physics Department, Igor Sikorsky Kyiv Polytechnic Institute
(37, Prosp. Beresteiskyi, Kyiv 03056, Ukraine)

SPHERICALLY SYMMETRIC CONFIGURATIONS IN THE DARK MATTER MODEL WITH LIGHT SCALARON

Static spherically symmetric (SSS) solutions of the quadratic $f(R)$ gravity are studied in the Einstein's frame under conditions of asymptotic flatness. Following recent dark matter model, we consider the scalaron mass of the order of several meV. We found a representation of the basic equations that enabled us to perform a numerical investigation of the SSS configurations with sufficiently large (astrophysically relevant) masses. There is always a region around the center with significant effects due to a (nontrivial) scalaron field. The size of this region can be essentially larger than the Schwarzschild radius of the configuration. We describe asymptotic regimes near the naked singularity at the center and at spatial infinity and relate the parameters of these regimes.

K e y w o r d s: compact astrophysical objects, modified gravity, scalar fields.

1. Introduction

Recently, a new view of dark matter (DM) as light scalaron has been proposed [1], which continues the line of DM models using $f(R)$ gravity [2–8] that is the most direct modification of the General Relativity (see [9–11] for reviews). In this theory, the gravitational Einstein–Hilbert Lagrangian density is replaced by a more general function $f(R)$ of the scalar curvature R. This leads to fourth-order equations with respect to the space-time metric $g_{\mu\nu}$ (Jordan frame). However, in a number of the $f(R)$ versions, it is possible to reduce the problem to usual Einstein equations [9–11] with respect to new metric $\hat{g}_{\mu\nu}$ (Einstein frame) by means of the conformal transformation

$$\hat{g}_{\mu\nu} = e^{2\xi} g_{\mu\nu}, \tag{1}$$

where some scalar field ξ dubbed a scalaron [1] satisfies an additional nonlinear wave equation that involves a scalaron mass μ.

Natural questions arise about the possible role of the $f(R)$ gravity in compact astrophysical objects. Most publications on this subject deal with the black-hole configurations [13–17]. The static spherically symmetric (SSS) systems without a horizon have been investigated numerically in [12, 18].

[1] In fact, the canonical scalaron is obtained by some rescaling of ξ. However, following [12], we prefer to use the dimensionless ξ. This explains multipliers in the scalaron potential below.

Citation: Zhdanov V.I. Spherically symmetric configurations in the dark matter model with light scalaron. *Ukr. J. Phys.* **70**, No. 11, 753 (2025). https://doi.org/10.15407/ujpe70.11.753.

In the case of astrophysical objects, the total mass M of the astrophysical configuration can be combined with the scalaron mass μ to yield a dimensionless (in geometrized units [2]) parameter $M\mu$. The DM model [1] deals with comparatively small scalaron mass ∼4 meV (see also [2, 5–8]) consistent with the experimental lower limit [3, 19–21]. Nevertheless, in astrophysical objects, the value of $M\mu$ is quite large: e.g., for the Solar mass systems $\mu M \sim 3 \times 10^9$ and, for typical masses of central objects in active galactic nuclei, $\mu M \sim 10^{18} \div 10^{19}$. This creates some troubles in the numerical simulations because of exponentially large numbers. Note that the numerical results obtained in [12, 18] in the case of the quadratic $f(R)$ model deal only with modest $M\mu$.

In this paper, we will consider properties of SSS solutions for sufficiently large $M\mu$. We consider the scalaron potential arising in the Einstein's frame of the quadratic $f(R)$ gravity as in the Starobinsky work [22], see also [1, 12, 18].

This paper is organized as follows. In Section 2, we review the relations of $f(R)$ gravity in the Einstein's frame for SSS configurations, known from earlier publications. The basic equations in a form suitable for numerical simulations in the case of large $M\mu$ are presented in Section 3. In Section 4, we perform numerical calculations to illustrate the solutions. In Section 5, we discuss our results.

2. Basic Equations in the Einstein Frame

In the DM model of [1], the quadratic $f(R)$ allows for transition to the Einstein frame by means of transformation (1). The corresponding scalaron self-interaction potential $W(\xi)$ is [3, 22]

$$W(\xi) = \mu^2 w(\xi), \quad w(\xi) = \frac{3}{4}\left(1 - e^{-2\xi}\right)^2. \tag{2}$$

For the SSS space-time, we use the Schwarzschild coordinate system (curvature coordinates) with

$$d\hat{s}^2 \equiv \hat{g}_{\mu\nu} dx^\mu dx^\nu = e^\alpha dt^2 - e^\beta dr^2 - r^2 dO^2, \tag{3}$$

where $r > 0$, $\alpha \equiv \alpha(r)$, $\beta \equiv \beta(r)$ and $dO^2 = d\theta^2 + \sin^2\theta d\varphi^2$ stands for the metric element on the unit sphere.

[2] $c = \hbar = 8\pi G = 1$; the metric signature is $(+\,-\,-\,-)$.

In the absence of non-gravitational fields, the nontrivial equations for the static metric (3) in the Einstein's frame are as follows [12]

$$\frac{d}{dr}(\alpha + \beta) = 6r\left(\frac{d\xi}{dr}\right)^2, \tag{4}$$

$$\frac{d}{dr}(\alpha - \beta) = -\frac{2}{r} + \frac{2e^\beta}{r}[1 - r^2 W(\xi)]. \tag{5}$$

where $\xi \equiv \xi(r)$. Equations (4), (5) for α and β must be supplemented by an equation for the scalaron [12]:

$$\frac{d}{dr}\left[r^2 e^{\frac{\alpha-\beta}{2}} \frac{d\xi}{dr}\right] = \frac{r^2}{6} e^{\frac{\alpha+\beta}{2}} W'(\xi). \tag{6}$$

In an asymptotically flat static space-time, it is assumed that, for $\xi(r) \to 0$, Eq. (6) can be well approximated by the equation for the linear massive scalar field on the Schwarzschild background

$$\exp[\alpha(r)] = 1 - r_g/r, \quad \exp[\beta(r)] = (1 - r_g/r)^{-1}, \tag{7}$$

where $r_g = 2M$, where $M > 0$ is the configuration mass. The asymptotics (7) hold true as long as $\xi \to 0$ approaches zero sufficiently rapidly for $r \to \infty$. However, this is not enough to determine the unique solution of system (4),(5),(6) and additional information about $\xi(r)$ is needed. For large r, small $\xi(r)$ must decay exponentially [23–25] with the asymptotic behavior

$$\xi(r) = Q\left(\frac{r_g}{r}\right)^{1+M\mu} e^{-\mu r}. \tag{8}$$

The constant Q, which characterizes the strength of the scalar field at infinity, will be called the scalar charge. For given M and Q, the asymptotic formulas (7), (8) determine the solution in a unique way [12].

In what follows, we will restrict ourselves to positive ξ where the potential has a plateau-like form; this is preferable for physical reasons, which is preferable for physical reasons and agrees with current observational data [26] (see, e.g., [27])

3. Reduction of Equations

After introduction of the variable $x = \mu r$ Eqs (4),(5), (6)) can be rewritten as

$$\frac{d\chi}{dx} = 3x\left(\frac{d\xi}{dx}\right)^2, \quad \chi = \frac{1}{2}(\alpha + \beta); \tag{9}$$

$$\frac{d}{dx}\frac{\alpha - \beta}{2} = -\frac{1}{x} + \frac{e^\beta}{x}\left[1 - x^2 w(\xi)\right]; \tag{10}$$

$$\frac{d}{dx}\left[x^2 e^{\frac{\alpha-\beta}{2}}\frac{d\xi}{dx}\right] = \frac{x^2}{6}e^{\chi}w'(\xi). \quad (11)$$

This system does not involve μ, however, this parameter is still present in the boundary conditions for $x \to \infty$.

From rigorous analytic considerations in the case of a monotonous function $w(\xi)$, $\xi > 0$ [12] (cf. also the case of a minimally coupled scalar field [28]), it follows that, in any non-trivial case, there must be some "scalarization region", where the solution is essentially different from the Schwarzschild one, and it is possible to see a smoking gun of the modified gravity. In the case of a non-trivial scalaron, there is a naked singularity at the center [12].

We will focus on the astrophysically interesting case where the size of this region is large enough, say, $\sim 100 r_g$. On the other hand, there must be an interval of small exponentially decaying $\xi(r)$ for $r \geq r_0$ (8); the metric in this region quickly takes on the Schwarzschild values (7) as r grows. This will be labeled as interval A.

For large $M\mu$, it is difficult to perform direct numerical integration of system (9), (10), (11) for all $r > 0$ because of exponentially large numbers involved and occurrence of rapid changes during transition from the scalarization region to A. In this regard, we proceed separately for $r > r_0$ and for $r < r_0$, where r_0 denotes the lower bound of A. We use an analytic approximation for $r > r_0$ and continue to numerically move to other regions with decreasing $r \in (0, r_0)$. Backward integration is preferable here, because it avoids exponentially growing errors in the calculations.

Let $\xi_0 \equiv \xi(r_0)$ is sufficiently small, so as to use formulas (7), (A.6) for $r \geq r_0$. For given $\xi(r_0)$, the value of r_0 can be related to the scalar charge according to (25). In order to consider the problem for large $M\mu$, we introduce a new independent variable p by means of the relations

$$x = r\mu = X_0 + \frac{p}{X_0} \equiv X_0 U(p), \quad U(p) = 1 + \frac{p}{X_0^2}, \quad (12)$$

where $X_0 = \mu r_0 \gg 1$ and the interval $r \in (0, r_0]$ corresponds to negative $p \in (-X_0^2, 0]$. We will move from $p = 0$ to negative values.

Equation (9) yields

$$\frac{d\chi}{dp} = 3U\left(\frac{d\xi}{dp}\right)^2 X_0^2, \quad (13)$$

Denote

$$Y = U\exp\left(\frac{\alpha-\beta}{2}\right), \quad Z = -X_0 U Y \frac{d\xi}{dp}. \quad (14)$$

After the transition to the new variable, Eq. (5) multiplied by $\exp[(\alpha-\beta)/2]$ can be transformed to

$$\frac{dY}{dp} = e^{\chi}\left[\frac{1}{X_0^2} - U^2 w(\xi)\right]. \quad (15)$$

Using (12), (14), from equation (6) we get

$$\frac{d}{dp}\left[UY\frac{d\xi}{dp}\right] = \frac{U^2}{6X_0^2}e^{\chi}w'(\xi). \quad (16)$$

and (16) is reduced to two first-order equations

$$\frac{d\xi}{dp} = -\frac{Z}{X_0 UY}, \quad (17)$$

$$\frac{dZ}{dp} = -\frac{U^2}{6X_0}e^{\chi}w'(\xi). \quad (18)$$

Substitution of (17) into (13) yields

$$\frac{d\chi}{dp} = \frac{3Z^2}{UY^2}. \quad (19)$$

Now, we have a closed system of four equations (15), (17), (18), (19) in a normal form, which is ready for the backwards numerical integration, starting from $p = 0$. Correspondingly, we set initial data at $p = 0$, which corresponds to $r = r_0 > r_g$:

$$\begin{aligned} &\xi(0) = \xi_0, \quad Y(0) \equiv Y_0 = \exp\left[\frac{\alpha_0 - \beta_0}{2}\right], \\ &\chi(0) = \chi_0, \quad Z_0 = -X_0 Y_0\left(\frac{d\xi}{dp}\right). \end{aligned} \quad (20)$$

From (A.5)

$$Z_0 = -X_0 Y_0\left(\frac{d\xi}{dp}\right)_0 = \xi_0 \exp(\alpha_0/2). \quad (21)$$

Following [12, 28], from (9)–(11) we infer that there exist limits

$$Y_C = \lim_{r\to 0} Y(r), \quad Z_C = \lim_{r\to 0} Z(r), \quad (22)$$

which define the asymptotic behavior of $\alpha(r)$, $\beta(r)$ and $\xi(r)$ for $r \to 0$

$$\begin{aligned} &\alpha(r) \sim (3\eta^2 - 1)\ln(r/r_g), \\ &\beta(r) \sim (3\eta^2 + 1)\ln(r/r_g), \\ &\xi(r) \sim -\eta\ln(r/r_g), \end{aligned} \quad (23)$$

where $\eta = X_0 Z_C / Y_C$.

4. Numerical Calculations

In the case of the scalaron potential of the quadratic model (2), we consider the positive branch of $\xi > 0$.

The initial conditions at r_0 must be agreed with the consitions of asymptotic flatness. The value ξ_0 must satisfy inequality (A.8) in order that the weak-field approximation (8) can be used. Therefore, in the numerical simulations we impose initial conditions as follows

$$\xi(r_0) = \frac{\tilde{\xi}_0}{\sqrt{X_0}}, \tag{24}$$

where $\tilde{\xi}_0 \ll 1$ is fixed.

Using (8) one can relate r_0 with Q. For $r_0 \gg \gg r_g$, on account of (24), after neglecting the term $\sim O(\ln(\mu r_0))/(M\mu)$ we get simple relation in the limit of large $M\mu$

$$q = \frac{\ln Q}{\mu r_g} = \left(\frac{r_0}{r_g}\right) + \frac{1}{2}\ln\left(\frac{r_0}{r_g}\right). \tag{25}$$

We treated system (15), (17), (18), (19) numerically for different $M\mu$ and various sizes of the scalarization region. Typical examples are shown in Figs. 1–5 for two values of q (25): $q = 50$ corresponding to $r_0/r_g = 113$ and $q = 100$ corresponding to $r_0/r_g = 228$; we typically used $\tilde{\xi}_0 = 0.001$ in (24).

An important role in describing the qualitative properties of solutions is due to functions $Y(r)$ and $Z(r)$. In region C the curves $Y(r)$ and $Z(r)$ for $r \lesssim r_0/2$ are flattened and $Y(r) \approx Y_C$, $Z(r) \approx \approx Z_C$. This is clearly visible in Figs. $Y(r)$ and $Z(r)$, which define the main (logarithmic) terms in asymptotics 1 and for 2); it is ensured by the rapid decrease of $e^{\chi} \approx e^{\beta}$ as r decreases (see Figs. 3, 4). It is important to note very weak dependencies $\alpha(r)$ and

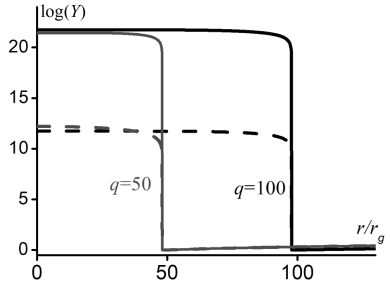

Fig. 1. $\log Y(r)$ against r/r_g for $q = 50$, 100 (correspondingly, $r_0 = 48.0$, 97.7). Solid lines: $\log(M\mu) = 20$; dashed: $\log(M\mu) = 10$. Outside the scalarization region there is a slight increase of $Y(r) \approx (r - r_g)/r_0$, but this is not visible in this figure

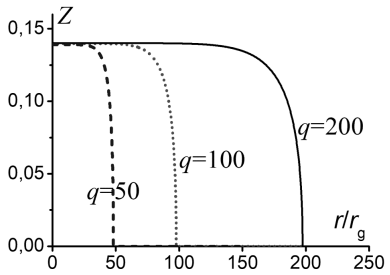

Fig. 2. $Z(r)$ against r/r_g for $q = 50, 100, 200$ (correspondingly, $r_0 = 48.0$, 97.7, 197.4). Outside the scalarization region, $Z(r) > 0$ tends to zero. For fixed q, in the scalarization region, the curves Z(r) look practically the same for different $\log(M\mu) = 3 \div 20$

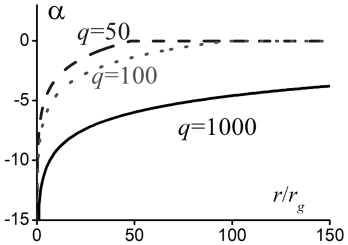

Fig. 3. $\alpha(r)$ against r/r_g for $q = 50, 100, 1000$ (correspondingly, $r_0 = 48.0$, 97.7, 996.5). The curves look practically the same for $\log(\mu M) = 3 \div 20$. Outside the scalarization region $\alpha(r) \approx -r_g/r$

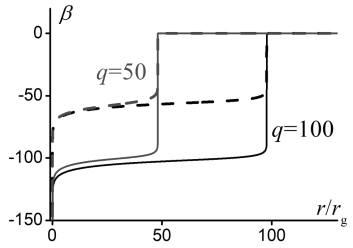

Fig. 4. $\beta(r)$ against r/r_g. The parameters and line styles are the same as in Fig. 1. Outside the scalarization region $\beta(r) \approx \approx r_g/r$

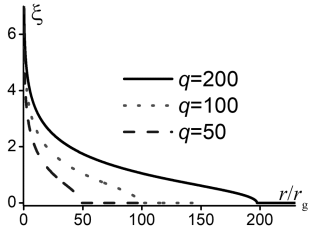

Fig. 5. $\xi(r)$ against r/r_g for $q = 50$, 100, 200. The curves look the same for $\log(\mu M) = 3 \div 20$. Outside the scalarization region, $\xi(r)$ is approximately given by (8)

$Z(r)$, on $\log(M\mu) \in [3, 20]$. The behavior of $\xi(r)$ is shown in Fig. 5.

5. Discussion

We have found a representation of the basic equations describing SSS configurations in the Einstein frame of the quadratic $f(R)$ gravity, which allowed us to perform numerical calculations for rather high values of $M\mu$, up to 10^{20}. This can be used in the case of the DM model (e.g., [1, 3]) with scalaron mass from the meV range satisfying the existing experimental lower limits [19, 20]. The results are as follows.

For arbitrary non-trivial [3] $\xi(r)$ there are three main regions of the radial variable with different types of behavior of the solutions. There is some value r_0 of the radial variable that separates regions of the weak and strong scalaron fields ξ. For $r \geq r_0$ (region A), we have small $\xi(r)$ that decays exponentially according to (8) as r grows. The metric takes on the Schwarzschild values. This behavior is common for a number of models that describe a massive linear scalar field equation in the weak-field regime on the Schwarzschild background.

On the other hand, for smaller r (roughly $r \lesssim r_0/2$, region C), the dependencies $Y(r)$ and $Z(r)$, defined in (14), are flattened and have a non-zero limits for $r \to 0$ (see Figs. 1 and 2). In this region, we have practically constant values of these functions and of $rd\xi/dr$. It is known [12] that there is a naked singularity at the center for any $\xi(r) \not\equiv 0$. Note that the existence of limits (22) and the behavior near the center is typical of a wide class of SSS solutions with scalar field [28].

In the intermediate region (B), there is an abrupt change in the metric near r_0. Then, as r decreases, the solution smoothly enters mode C. It is important that the functions $Y(r)/X_0$ and $Z(r)$ are practically independent of $M\mu$ for fixed q. This has been confirmed numerically for $\log(M\mu) = 5 \div 20$.

In the scalarization region defined by r_0 there are significant effects due to the scalaron field that may affect the structure of accretion disk around the singularity at the center. The size of this region may be significant depending on q and/or Q parameter. This can be used to deny or confirm the existence of such configurations from observations.

[3] The case $\xi = 0$ corresponds to the Schwarzschild solution in Einstein and Jordan frames.

Our findings deal with solutions of the $f(R)$ gravity in the Einstein frame. Transition to the Jordan frame is performed according to (1) yielding the vacuum solutions. In the Einstein frame this corresponds to the "scalar vacuum,", when we have the Einstein equations for the conformally transformed metric with the energy-momentum tensor of scalaron scalar field [9–11]. However, our results can be applied in the case where a non-zero spherically symmetric continuous mass-energy distribution in the central region is present. In this case, the gravitational field in the inner region is determined by the energy-momentum tensor inside the body. Outside this body, we have the above vacuum solution, defined by the total mass M and the "scalar charge" Q, which, however, depends on the appropriate matching with the inner region.

I am grateful to Yu. Shtanov and O. Stashko for useful discussions. This work was partially supported by the National Research Foundation of Ukraine under project No. 2023.03/0149.

APPENDIX

Approximate solutions in the region A

For $|\xi| \ll 1$ the scalaron potential is approximately $W(\xi) = 3\mu^2\xi^2$ and Eq. (6) describes linear scalar field

$$\frac{d}{dr}\left[r^2 e^{\frac{\alpha-\beta}{2}}\frac{d\xi}{dr}\right] = \mu^2 r^2 e^{\frac{\alpha+\beta}{2}}\xi. \tag{A.1}$$

For large $M\mu \gg 1$, we can apply the WKB method. Substituting $\xi(r) = \exp(\mu u)$ into (A.1) we have

$$\left(\frac{du}{dr}\right)^2 + \frac{1}{\mu}\frac{d^2u}{dr^2} + \frac{1}{\mu}\left[\frac{d}{dr}\left(2\ln r + \frac{\alpha-\beta}{2}\right)\right] = e^{\beta}. \tag{A.2}$$

Putting $u(r) = u_0(r) + \mu^{-1}u_1(r) + ...$ in zeroth order in μ^{-1} leads to

$$\frac{du_0}{dr} = -e^{\beta/2}, \tag{A.3}$$

where we considered the asymptotic behavior at the infinity. In the next order

$$u_1(r) = -\ln r - \alpha/4 + \text{const}. \tag{A.4}$$

up to terms of the order of $(M\mu)^{-1}$.

Using (A.3) yields

$$\frac{d\xi}{dr} = -\mu\xi e^{\beta/2}\left[1 + O\left(\frac{1}{M\mu}\right)\right]. \tag{A.5}$$

For $M\mu \gg 1$, $r > 2r_g$ and $\xi \ll 1$, in case of the Schwarzschild metric (7), equations (A.3), (A.4) yield

$$\xi(r) = \frac{Q(4/e)^{M\mu}\exp\left(-\mu r\sqrt{1-\frac{r_g}{r}}\right)}{\left(1-\frac{r_g}{r}\right)^{1/4}\left(1+\sqrt{1-\frac{r_g}{r}}\right)^{\mu r_g}}\left(\frac{r_g}{r}\right)^{1+M\mu}, \tag{A.6}$$

which is true up to terms of order $(M\mu)^{-1}$. This formula leads to (8) for $r \gg r_g$,

The approximations are effective provided that ξ is small enough not affect the metric via (4),(5). Therefore, we must estimate how $\xi(r)$ affects $\alpha(r)$ and $\beta(r)$ under the conditions of the asymptotic flatness. We assume here $r \gg r_g$. Using (7) as zeroth approximation, the first order correction to $\chi(x)$ is obtained from (4) taking into account either (8) or (A.6)

$$\chi(r) = -3\int\limits_r^\infty dr' r' \left(\frac{d\xi}{dr}\right)^2 \approx -\frac{3}{2}\mu r \xi^2(r). \tag{A.7}$$

Therefore, in order that $|\chi_0| \ll 1$, one must have

$$X_0 \xi_0^2 \ll 1. \tag{A.8}$$

Also, under condition (A.8) one can infer from (5) that $|e^{-\alpha_0}(1 - r_g/r_0) - 1| \ll 1$, $|e^{\beta_0}(1 - r_g/r_0) - 1| \ll 1$. In this case one can be sure that for $r \geq r_0$ we can use formulas (7) and (A.6).

1. Y. Shtanov. Light scalaron as dark matter. *Phys. Lett. B* **820**, 136469 (2021).
2. S. Capozziello, V.F. Cardone, A. Troisi. Dark energy and dark matter as curvature effects. *J. Cosmol. Astropart. Phys.* **08**, 001 (2006).
3. J.A.R. Cembranos. Dark matter from R2 gravity. *Phys. Rev. Lett.* **102**, 141301 (2009).
4. C. Corda, H.J. Mosquera Cuesta, R. Lorduy Gomez. High-energy scalarons in R2 gravity as a model for Dark Matter in galaxies. *Astropart. Phys.* **35**, 362 (2012).
5. T. Katsuragawa, S. Matsuzaki. Dark matter in modified gravity. *Phys. Rev. D* **95**, 044040 (2017).
6. T. Katsuragawa, S. Matsuzaki. Cosmic history of chameleonic dark matter in $F(R)$ gravity. *Phys. Rev. D* **97**, 064037 (2018); Erratum: *Phys. Rev. D* **97**, 129902 (2018).
7. B.K. Yadav, M.M. Verma. Dark matter as scalaron in $f(R)$ gravity models. *J. Cosmol. Astropart. Phys.* **10**, 052 (2019).
8. N. Parbin, U.D. Goswami. Scalarons mimicking dark matter in the Hu–Sawicki model of $f(R)$ gravity. *Mod. Phys. Lett. A* **36**, 2150265 (2021).
9. T.P. Sotiriou, V. Faraoni. f(R) theories of gravity. *Rev. Mod. Phys.* **82**, 451 (2010).
10. A. De Felice, S. Tsujikawa. $f(r)$ theories. Liv. Rev. Relativ. **13**, 3 (2010).
11. S. Nojiri, S.D. Odintsov, V.K. Oikonomou. Modified gravity theories on a nutshell: Inflation, bounce and late-time evolution. *Phys. Rep.* **692**, 1 (2017).
12. V.I. Zhdanov, O.S. Stashko, Y.V. Shtanov. Spherically symmetric configurations in the quadratic $f(R)$ gravity. *Phys. Rev. D* **110**, 024056 (2024).
13. A. de La Cruz-Dombriz, A. Dobado, A.L. Maroto. Black holes in $f(R)$ theories. *Phys. Rev. D* **80**, 124011 (2009).
14. S. Bhattacharya. Rotating Killing horizons in generic $F(R)$ gravity theories. *Gen. Relativ. Gravit.* **48**, 128 (2016).
15. P. Canate. A no-hair theorem for black holes in $f(R)$ gravity. *Class. Quant. Gravity* **35**, 025018 (2017).
16. G.G.L. Nashed, S. Nojiri. Nontrivial black hole solutions in $f(R)$ gravitational theory. *Phys. Rev. D* **102**, 124022 (2020).
17. G.G.L. Nashed, S. Nojiri. Specific neutral and charged black holes in $f(R)$ gravitational theory. *Phys. Rev. D* **104**, 124054 (2021).
18. E. Hernandéz-Lorenzo, C.F. Steinwachs. Naked singularities in quadratic $f(R)$ gravity. *Phys. Rev. D* **101**, 124046 (2020).
19. D.J. Kapner, T.S. Cook, E.G. Adelberger, J.H. Gundlach, B.R. Heckel, C.D. Hoyle, H.E. Swanson, Tests of the gravitational inverse-square law below the dark-energy length scale. *Phys. Rev. Lett.* **98**, 021101 (2007).
20. E.G. Adelberger, B.R. Heckel, S.A. Hoedl, C.D. Hoyle, D.J. Kapner, A. Upadhye. Particle-physics implications of a recent test of the gravitational inverse-square law. *Phys. Rev. Lett.* **98**, 131104 (2007).
21. J.A.R. Cembranos, Modified gravity and dark matter. *J. Phys. Conf. Ser.* **718**, 032004 (2016).
22. A.A. Starobinsky. A new type of isotropic cosmological models without singularity. *Phys. Lett. B* **91**, 99 (1980).
23. R.A. Asanov. Static scalar and electric fields in Einstein's theory of relativity. *Zh. Èksp. Teor. Fiz.* **26**, 424 (1968).
24. R.A. Asanov. Point source of massive scalar field in gravitational theory. *Theor. Mat. Phys.* **20**, 667 (1974).
25. D.J. Rowan, G. Stephenson. The massive scalar meson field in a Schwarzschild background space. *J. Phys. A* **9**, 1261 (1976).
26. Y. Akrami *et al.* (Planck Collaboration). Planck 2018 results. X. Constraints on inflation. *Astron. Astrophys.* 641, A10 (2020).
27. Y. Shtanov, V. Sahni, S.S. Mishra. Tabletop potentials for inflation from $f(R)$ gravity. *J. Cosmol. Astropart. Phys.* **03**, 023 (2023).
28. V.I. Zhdanov, O.S. Stashko. Static spherically symmetric configurations with N nonlinear scalar fields: Global and asymptotic properties. *Phys. Rev. D* **101**, 064064 (2020).

Received 12.03.25

В.І. Жданов

СФЕРИЧНО-СИМЕТРИЧНІ КОНФІГУРАЦІЇ В МОДЕЛІ ТЕМНОЇ МАТЕРІЇ ЗІ ЛЕГКИМ СКАЛЯРОНОМ

Досліджено статичні сферично-симетричні (ССС) розв'язки квадратичної $f(R)$-гравітації в системі Айнштайна за умов асимптотичної площинності. Згідно з нещодавньо запропонованою моделлю темної матерії, ми розглядаємо величину маси скалярона порядку кількох меВ. Знайдено представлення основних рівнянь, яке дозволило провести чисельне дослідження ССС конфігурацій з достатньо великими (астрофізично прийнятними) масами. Показано, що навколо центра симетрії завжди є область зі значними ефектами завдяки ненульовому полю скалярона. Розмір цієї області може бути значно більшим, ніж радіус Шварцшильда ССС конфігурації. Отримано асимптотичні режими поблизу голої сингулярності в центрі і на просторовій нескінченності та оцінено параметри цих режимів.

Ключові слова: компактні астрофізичні об'єкти, модифікована гравітація, скалярні поля.